AHC: An integrated numerical model for simulating agroecosystem processes—model description and application

Annex A. Evaporation, transpiration and surface ponding

Annex B. Description of nitrogen transformation and the equations

Annex C. EPIC crop growth module

Annex D. Treatment for soil frost and thaw conditions

Annex E. Treatment of bottom boundary conditions and lateral drainage

Annex F. Supplementary material for the salinity and nitrogen cases

Annex A. Evaporation, transpiration and surface ponding

(1) ***Evaporation and transpiration under stress***

The calculation of potential evapotranspiration (ET_p, mm d^{-1}) and its partitioning to crop transpiration rate (T_p, mm d^{-1}) and soil evaporation rate (E_p, mm d^{-1}) are kept same as in the original SWAP model (Kroes and van Dam, 2003). ET_p is estimated by the Penman-Monteith equation (Monteith, 1965) using daily meteorological data of solar radiation, air temperature, relative humidity and wind speed as well as crop parameters described below. The method for reducing T_p and E_p to the lower actual transpiration and evaporation rates is modified and thus different from the SWAP.

The potential soil evaporation rate of a wet, bare soil, E_{p0} (cm d^{-1}), is computed using Penman-Monteith equation with a crop resistance (r_c) 0 s m^{-1} and a crop height 0.1 cm. Then model calculates a daily average of the potential soil evaporation rate, E_p (cm d^{-1}), as follows (Goudriaan, 1977; Belmans et al., 1983):

$$E_p = E_{p0} \cdot e^{-k_{gr} LAI} \tag{A1}$$

where k_{gr} (-) is the extinction coefficient for global solar radiation, and LAI (-) is the leaf area index. Under dry soil conditions, the maximum evaporation rate, E_{max} (cm d^{-1}), is first calculated according to the Darcy's law (van Dam et al., 1997). Since the Darcy's law can overestimate E_a, three functions which proposed by Black et al. (1969), Boesten and Stroosnijder (1986) and Allen et al. (1998), respectively, are optionally applied to limit actual evaporation (noted as E_{alim}, cm d^{-1}). The former two functions are empirical exponential functions that have been adopted by the SWAP and described in Kroes and van Dam (2003). However, the calculation of E_{alim} in the two functions is only related to the rainfall and time but not to the surface soil moisture. Thus, this implies that the calibrated functions would still result in an under- or over-estimation of soil evaporation when different upward flux from lower soil layers exists, such as under conditions of shallow water tables (Xu et al., 2015). The third function uses a mechanism two-stage approach, with equation of $E_{alim}=K_r E_p$. The evaporation reduction coefficient K_r is calculated as a function of soil water content of surface layer, as follows:

$$\begin{cases} K_r = 1 & \text{for energy stage} \\ K_r = \dfrac{e^{f_k \cdot W_{rel}} - 1}{e^{f_k} - 1} & \text{for falling stage, } 0 \le K_r \le 1 \end{cases} \tag{A2}$$

where f_k is a decline factor (-) and W_{rel} (-) is the relative water content of the soil layer through which water moves to the evaporating soil surface layer (i.e., upper soil layer with thickness $Z_{e,top}$). $Z_{e,top}$ is assigned to 15 cm and expands to a maximum depth (15-50 cm) when W_{rel} drops below a threshold of 0.4 (Raes et al., 2012). The third function is more general and recommended especially for the shallow water table conditions. Finally, the AHC determines the actual evaporation rate (E_a, cm d^{-1}) by taking the minimum value of E_p, E_{max} and E_{alim}.

In addition, the effect of mulches on soil evaporation can be considered to further limit the evaporation loss in the AHC. It is described by two factors, i.e., the fraction of soil surface covered by mulch (CF_{mul}, -) and adjusted factor of mulch material (f_{mm}, -) (Allen et al., 1998). The E_a is then adjusted with multiplying by a mulching reduction coefficient ($K_{r,mul}$, -) that is calculated as follows:

$$K_{r,mul} = 1 - CF_{mul} \cdot f_{mm} \tag{A3}$$

where CF_{mul} varies from 0 to 100%, and f_{mm} varies between 0.5 for mulches of plant material and is close to 1.0 for plastic mulches. The adjustment is not applied when standing pond water remains on the soil surface.

The ET_p of a canopy completely covering the soil is calculated using the Penman-Monteith equation. In case of a wet canopy, the r_c is set to zero. In case of a dry crop with optimal water supply in the soil, r_c is minimal and varies between 30 s m^{-1} for arable crop to 150 s m^{-1} for trees in a forest (Allen et al., 1989). Then, a daily average of the potential transpiration rate, T_p (cm d^{-1}), is obtained by:

$$T_p = (1.0 - W_{frac})ET_p - E_p \tag{A4}$$

where W_{frac} (-) is the fraction of the day that crop is wet, i.e., the ratio of the daily amount of intercepted precipitation to the ET_p rate of a wet canopy. The actual transpiration (T_a, cm d^{-1}) is governed by the root water uptake ($S_a(z)$, d^{-1}) which is calculated from the potential transpiration, rooting depth and distribution and a possible reduction due to water and salt stress, as follows:

$$S_a(z) = \alpha_{ws}\frac{T_p}{z_{root}} = \alpha_w \alpha_s \frac{T_p}{z_{root}} \tag{A5}$$

where α_w (-) and α_s (-) are the reduction coefficients relative to water stress and salt stress, respectively, α_{ws} (-) is the reduction coefficients of integrated water-salt stress, and z_{root} is the rooting depth (cm). A homogeneous root length density distribution is adopted over the rooting depth as often assumed in the modeling practice, because the distribution is usually not available (Kroes and van Dam, 2003).

In the original SWAP model, the stress coefficients α_{w} and α_{s} are described by a reduction function proposed by Feddes et al. (1978) and Maas and Hoffman (1977), respectively. In the AHC, the S-shaped functions suggested by van Genuchten (1987) are provided as well to calculate the water and salt stress. In addition, a salinity threshold value suggested by Dirksen and Augustijn (1988) is adopted to better describe the salinity stress, as follows:

$$\alpha_s(h_o) = \frac{1}{1+((h_o^* - h_o)/(h_o^* - h_{o50}))^p} \tag{A6}$$

where h_o is the soil solution osmotic head (cm), h_o^* is the threshold value of osmotic head (cm), h_{o50} is the soil solution osmotic head of soil salinity at which $\alpha_s(h_o)$ is reduced by 0.50 (cm), and p is an empirical crop, soil and climate-specific dimensionless parameter described as (Homaee et al., 2002):

$$p = \frac{h_{o50}}{h_{o50} - h_o^*} \tag{A7}$$

Eq. (A6) is based on the soil solution osmotic head instead of the electrical conductivity of saturation extracts (EC_e). If h_o^* is equal to 0 and p is just a user-specified parameter, Eq. (A6) becomes the S-shaped function as same as that proposed by van Genuchten (1987) for calculating the salinity stress. The S-shaped models could provide sufficient flexibility without introducing unwarranted complexity.

The AHC also includes the function of the compensated root water uptake. A critical value of the water stress index ω_c, i.e., a root adaptability factor, is further introduced to describe the compensated water uptake, referring to Jarvis (1989). ω_c represents a threshold value, above which the root water uptake reduced in stressed parts of the root zone is fully compensated for by uptake from other less-stressed parts (Eq. A8). The stress parts are just partly compensated if α_{ws} is below this critical value (Eq. A9).

$$T_a^* = \sum_{i=1}^{Nr} T_{a,i}^* = \sum_{i=1}^{Nr} \frac{T_{a,i}}{\alpha_{ws}} = \sum_{i=1}^{Nr} \frac{T_p A_i \alpha_{ws,i}}{\alpha_{ws}} = \frac{T_p}{\alpha_{ws}} \sum_{i=1}^{Nr} A_i \alpha_{ws,i} = \frac{T_p}{\alpha_{ws}} \alpha_{ws} = T_p, \qquad \alpha_{ws} \ge \omega_c \tag{A8}$$

$$T_a^* = \sum_{i=1}^{Nr} T_{a,i}^* = \sum_{i=1}^{Nr} \frac{T_{a,i}}{\omega_c} = \sum_{i=1}^{Nr} \frac{T_p A_i \alpha_{ws,i}}{\omega_c} = \frac{T_p}{\omega_c} \sum_{i=1}^{Nr} A_i \alpha_{ws,i} = \frac{\alpha_{ws}}{\omega_c} T_p, \qquad \alpha_{ws} \ge \omega_c \tag{A9}$$

where T_a^* and $T_{a,i}^*$ are the total T_a and the T_a for the i^{th} compartment, respectively, when considering the root water uptake compensation. N_r is the number of compartments in the root zone, $\alpha_{ws,i}$ is the reduction coefficients of the water-salt stress for the i^{th} compartment, and A_i (-) is the weight of water uptake distribution for the i^{th} compartment as a function of relative root length density and compartment thickness. A_i is normalized to ensure that A_i integrates to unity over the root zone.

(2) "Surface reservoir" boundary condition:

A "surface reservoir" boundary condition is applied if the surface ponding is expected to develop, as follows:

$$-K\left(\frac{\partial h}{\partial z}+1\right)=q_0(t)-\frac{dh_{pond}}{\partial t} \qquad \text{at } z=0 \tag{A10}$$

where q_0 is the net infiltration rate, i.e., the difference between precipitation and evaporation (cm d^{-1}), h_{pond} is the ponding depth of water (cm), q_{runoff} is the surface runoff (cm), z_{sill} is the maximum ponding height (cm), γ_{sill} is the runoff resistance (d), and β is an exponent (-).

If the ponding depth is greater than a threshold value, the surface runoff is supposed to happen and estimated as follows:

$$q_{runoff}=\frac{1}{\gamma_{sill}}\left(h_{pond}-z_{sill}\right)^{\beta_{sill}} \tag{A11}$$

where q_{runoff} is the surface runoff (cm), z_{sill} is the maximum ponding height (cm), γ_{sill} is the runoff resistance (d), and β is an exponent (-).

Annex B. Description of nitrogen transformation and the equations

(1) ***Mineralization and immobilization***

The concepts of mineralization and immobilization of nitrogen (N) are mainly adapted from the Daisy (Hansen, 2002) while also referring to the APSIM (McCown et al., 1996). The organic matter is divided into three main pools as follows: (1) soil organic matter is divided into two main pools, viz., dead soil organic matter (SOM) and microbial biomass (SMB); and (2) the added fresh organic matter (AOM) is defined as the third main pool. Each main pool is subdivided into two or three subpools with different decay rates. The SOM is similar as humus, and further subdivided into three subpools SOM_0, SOM_1 and SOM_2. The SOM_0 consists of almost inert soil organic matter. The active subpools SOM_1 and SOM_2 are assumed to consist of chemically and physically stabilized organic matter, respectively. Their decomposition rates are both simulated by first-order reaction kinetics (Eqs. B5 and B6). The active SOM pool is assumed to change from about 60% to 20% of total soil organic matter with depth increase for shallow soils (e.g., 0-60 cm) and 0-5% for deeper arable soils (McCown et al., 1996). The microbial biomass in the soil which usually accounts for less than 4% of the active humus is subdivided into two subpools designated SMB_1 and SMB_2, respectively. SMB_1 is considered to be more stable while SMB_2 is more dynamic part of the microbial biomass. The simulation of biomass turnover is based on growth efficiency, maintenance respiration and death rate coefficients, described using the first-order reaction kinetics equations (Eqs. B3 and B4) (Hansen et al., 1991). The AOM is the organic fertilizer such as plant residual, farmyard manure and slurry, which is allocated to the subpools AOM_1, AOM_2 and SOM_2. The subpools AOM_1 and AOM_2 are assumed to consist of mainly cell wall material and mainly water extractable cell material, respectively. Their decomposition rate of each subpool is calculated by first-order reaction kinetics (Eqs. B1 and B2). The SOM_2, SMB_2 and AOM_2 have a faster turnover compared with the SOM_1, SMB_1 and AOM_1.

$$\frac{dC_1}{dt} = C_0 f_0 - \alpha_1 k_1 C_1 \tag{B1}$$

$$\frac{dC_2}{dt} = C_0 f_{00} - \alpha_2 k_2 C_2 \tag{B2}$$

$$\frac{dC_3}{dt} = \alpha_1 k_1 C_1 E_1 f_1 + \alpha_5 k_5 C_5 E_5 + \alpha_6 k_6 C_6 E_6 \left(1 - f_6\right) - \alpha_3 k_3 C_3 - \alpha_3 \beta_1 C_3 \tag{B3}$$

$$\frac{dC_4}{dt} = \alpha_1 k_1 C_1 E_1 \left(1 - f_1\right) + \alpha_2 k_2 C_2 E_2 + \alpha_3 k_3 C_3 E_3 \left(1 - f_3\right) - \alpha_4 k_4 C_4 \left(2 f_4 - 1\right) - \alpha_4 \beta_2 C_4 \tag{B4}$$

$$\frac{dC_5}{dt} = \alpha_6 k_6 C_6 E_6 f_6 - \alpha_5 k_5 C_5 \tag{B5}$$

$$\frac{dC_6}{dt} = C_0 \left(1 - f_0 - f_{00}\right) + \alpha_3 k_3 C_3 E_3 f_3 + \alpha_4 k_4 C_4 E_4 f_4 - \alpha_6 \beta_6 C_6 \tag{B6}$$

where C_i is the carbon content of the i^{th} sub-pool (kg C ha^{-1}), k_i is a first-order decomposition rate coefficient which is modified according with the considered abiotic factors (kg C ha^{-1} d^{-1}), α_i is the stress factor for carbon turnover (-), f_i is partitioning coefficient for carbon flow (-), and E_i is the substrate utilization efficiency (-).

The soil temperature and moisture are two main abiotic factors influencing the above carbon turnover, while the clay content is a specific factor to SOM_1, SOM_2 and BOM_1. These factors are calculated for each soil compartment using Eqs. (B7)-(B10). It is assumed that there are no interaction effects between the different factors, and the combined effect is multiplicative (Hansen et al., 1991). Model allows flows of carbon among different subpools during the decomposition of the organic matter.

$$\alpha_1 = \alpha_2 = F_m(T) F_m(h) \tag{B7}$$

$$\alpha_3 = F_m(T) F_m(h) F_m(Clay) \tag{B8}$$

$$\alpha_4 = F_m(T) F_m(h) = \alpha_1 \tag{B9}$$

$$\alpha_5 = \alpha_6 = F_m(T)F_m(h)F_m(Clay) = \alpha_3 \quad \text{(B10)}$$

where T is the soil temperature (ºC), h is the soil water pressure head (cm), and $Clay$ is the clay content at the soil compartment (kg kg^{-1}). The stress function F_{m} (-) is calculated as follows:

$$F_m(T) = \begin{cases} 0 & T \le 0 \\ 0.1T & 0 < T \le 20 \\ \exp\left(0.47 - 0.027T + 0.00193T^2\right) & T > 20 \end{cases} \quad \text{(B11)}$$

$$F_m(h) = \begin{cases} 0.6 & h \ge -1 \\ 0.6 + 0.4\log\left(-h\right)/1.5 & -10^{1.5} \le h < -1 \\ 1.0 & -10^{2.5} \le h < -10^{1.5} \\ 1.0 - \log\left(-10^{-2.5}h\right)/4 & -10^{6.5} \le h < -10^{2.5} \\ 0 & h < -10^{6.5} \end{cases} \quad \text{(B12)}$$

$$F_m(T) = \begin{cases} 1.0 - aC_c & 0 < C_c \le C_c^{'} \\ 1.0 - aC_c^{'} & C_c > C_c^{'} \end{cases} \quad \text{(B13)}$$

where C_c' is set equal to 0.25 kg kg^{-1} and a is equal to 2.0.

The flows of matter between different pools are calculated in terms of carbon, and thus the corresponding nitrogen flows are calculated based on the carbon/nitrogen ratio (CNR) of the receiving pool. The CNR value is set constant for each subpool. A carbon balance for each pool of organic matter can be established resulting in an expression for the rate of change of carbon in each pool. As each pool of organic matter is characterized by a particular carbon to nitrogen ratio (CNR_i), an overall organic nitrogen balance can be established resulting in an equation for net mineralization of nitrogen as flows:

$$R_{\min} = -\sum_i CNR_i \frac{dC_i}{dt} \quad \text{(B14)}$$

(2) *Nitrification and NH_3 volatilization*

Nitrification is a microbial process related to the conversion of ammonia N to nitrate N, while NH_3 volatilization, the loss of ammonia to the atmosphere, often takes place simultaneously. They are estimated using a combination of the methods of Reddy et al. (1979) and Godwin et al. (1984) which are also adopted by EPIC model (Williams, 1995). This approach is based on the first-order kinetic equations (Reddy et al., 1979), described in Eqs. (B15)-(B27). The combined rate is first calculated using Eq. (B15), and then is partitioned into the nitrification and volatilization rates using the subsequent equations. Nitrification, the conversion of ammonia N to nitrate N, is regulated by the soil water content, temperature and pH. The volatilization, loss of ammonia to the atmosphere, is estimated simultaneously with nitrification. This loss from soil surface is affected by the soil temperature and wind speed, while that from subsurface soils is influenced by the depth, cation exchange capacity (CEC, cmol kg^{-1}) and soil temperature (Williams, 1995).

$$\frac{dWNH_4}{dt} = R_{nit+vol} = WNH_4\left[1-\exp\left(-k_{nit}-k_{vol}\right)\right] \tag{B15}$$

$$k_{\mathrm{nit}} = f_{\mathrm{T\_nit}} f_{\mathrm{sw\_nit}} f_{\mathrm{pH\_nit}} \tag{B16}$$

$$f_{\mathrm{T\_nit}} = 0.41\frac{T-5}{10} \qquad \mathrm{T_{soil}} > 5°C \tag{B17}$$

$$f_{\mathrm{sw\_nit}} = \begin{cases} \dfrac{SW-WP}{SW25-WP} & SW < SW25 \\ 1.0 & SW25 \le SW \le FC \\ 1.0-\dfrac{SW-FC}{PO-FC} & SW > FC \end{cases} \tag{B18}$$

$$f_{\mathrm{pH\_nit}} = \begin{cases} 0.307\mathrm{pH}-1.269 & \mathrm{pH} < 7.0 \\ 1.0 & 7.0 \le \mathrm{pH} \le 7.4 \\ 5.367-0.599\mathrm{pH} & \mathrm{pH} > 7.4 \end{cases} \tag{B19}$$

$$k_{\mathrm{vol}}=\begin{cases} f_{\mathrm{T\_nit}}\,f_{\mathrm{wind}} & \text{surface} \\ f_{\mathrm{T\_nit}}\,f_{\mathrm{CEC}}\,f_{\mathrm{depth}} & \text{subsurface} \end{cases} \tag{B20}$$

$$f_{\mathrm{wind}}=0.335+0.16\ln u_2 \tag{B21}$$

$$f_{\mathrm{CEC}}=\max\left(0.0,\ 1.0-0.038\mathrm{CEC}\right) \tag{B22}$$

$$f_{\mathrm{depth}}=1-\frac{1000x}{1000x+\exp(4.706-30.5x)} \tag{B23}$$

$$R_{\mathrm{nit}}=WNH_4\left[1-\exp\left(-k_{\mathrm{nit}}\right)\right] \tag{B24}$$

$$R_{vol}=WNH_4\left[1-\exp\left(-k_{vol}\right)\right] \tag{B25}$$

$$R_{vol}=R_{vol}\frac{R_{nit+vol}}{R_{nit}+R_{vol}} \tag{B26}$$

$$R_{nit}=R_{nit+vol}-R_{vol} \tag{B27}$$

where WNH_4 and WNO_3 are respectively NH_4-N and NO_3-N contents in the soil layer (kg N ha^{-1}), k_{nit} and k_{vol} are respectively the nitrification regulator for volatilization regulator (d^{-1}), R_{nit}, R_{vol} and $R_{nit+vol}$ are respectively the nitrification rate, volatilization rate and combined rate of nitrification and volatilization (kg N ha^{-1} d^{-1}), $f_{\mathrm{T\_nit}}$, $f_{\mathrm{sw\_nit}}$ and $f_{\mathrm{pH\_nit}}$ are respectively the factors of soil temperature, soil water and pH for N nitrification, f_{wind}, f_{depth} and f_{CEC} are respectively the factors of wind, soil depth and CEC for N volatilization (0-1), u_2 is the mean wind speed at 2 m height (m d^{-1}), x is the spatial coordinate assumed to be positive downward from soil surface (m), and PO is soil porosity (cm^3 cm^{-3}). SW is the soil water content of the soil layer (cm^3 cm^{-3}), WP and FC is the soil water content at plant wilting point and field capacity (cm^3 cm^{-3}), respectively, and $SW25$ is the soil water content at $WP+0.25(FC-WP)$

(cm^3 cm^{-3}).

(3) *Denitrification*

Nitrate N from nitrification or commercial fertilizer is subject to denitrification in anaerobic environments by microbes that are able to utilize the N in NO_3^- and NO_2^- as terminal electron acceptors. Denitrification is a complicated microbial process in which nitrate N is lost in the form of N_2 and N_2O gas from the soil to atmosphere. Soil denitrification is assumed to only take place in the top 20-cm soil layer. The denitrification rate is calculated using the first-order equation as a function of soil temperature and organic carbon content, as follows:

$$R_{den} = \begin{cases} WNO_3\left[1-\exp(-1.4 f_T OC)\right] & \mathrm{SWF} \geq 0.95 \\ 0 & \mathrm{SWF} < 0.95 \end{cases} \tag{B28}$$

$$f_{\mathrm{T\_den}} = 0.1 + 0.9\frac{T}{T+\exp(9.93-0.312T)} \tag{B29}$$

where R_{den} is the total denitrification rate (kg N ha^{-1} d^{-1}), OC is the percent content of soil organic carbon (%), and $f_{\mathrm{T\_den}}$ is the soil temperature factor for denitrification (0-1).

(4) *N₂O emission*

The nitrous oxide (N_2O) emitted from soils is an important part affecting stratospheric ozone levels and greenhouse effects. Both nitrification and denitrification contribute to the release of N_2O, which are both considered in the AHC. In nitrification, N_2O emission is estimated as a fraction of the nitrification rate, adjusted by the soil temperature and moisture (Eq. B30). N_2O emission during the denitrification process is calculated using Eq. (B32) for saturated and unsaturated conditions (Xu et al., 1998).

$$N_2O_{nit} = \alpha_{nit} R_{nit} f_{\mathrm{T\_nit}} f_{\mathrm{sw\_nit}} \tag{B30}$$

$$f_{sw\_den} = \exp\left(-23.77 + 23.77 wfps\right) \tag{B31}$$

$$N_2O_{den} = \begin{cases} 0.05 R_{den} & wfps \geq 1.0 \\ \alpha_{den} R_{den} (1 - f_{sw\_den}) & 0.8 \leq wfps < 1.0 \\ 0 & wfps < 0.8 \end{cases} \tag{B32}$$

where α_{nit} denotes the maximum fraction of nitrogen loss as N_2O through nitrification (-), f_{sw_den} is the soil moisture factor (-), *wfps* is the fraction of soil pore space filled with water (0-1), and α_{den} is the maximum fraction of the total denitrification rate R_{den} occurring as N_2O (-), with a default value of 0.5. α_{nit} is set at a default value of 0.002 and can also be calibrated from the field measurement. The fraction of N_2O lost in nitrification varies from 0.001 to 0.05 as reported by Goodroad and Keeney (1984).

(5) *Urea hydrolysis*

Urea is the major N fertilizer used for crop production in world agriculture. In the AHC, the rate for urea hydrolysis to ammonia ($HYDR_{urea}$, kg N ha^{-1} d^{-1}) is estimated using the first-order kinetics equation, referring to the WNMM model (Li et al., 2007):

$$HYDR_{urea} = WUREA\left[1.0 - \exp(-5.0 f_T wfps)\right] \tag{B33}$$

where *WUREA* is the urea content in the soil layer (kg N ha^{-1} d^{-1}). This implies that the urea hydrolysis is generally faster (2-3 days) in hot weather and wet soil while slower under cool and dry conditions (Li et al., 2007). This treatment is different from some other models (e.g., NLEAP and EPIC) which assume that the process of urea hydrolysis is so fast that the urea can be directly treated as NH_4^+as model input.

(6) *Plant N uptake*

The nitrogen uptake is estimated using a demand and supply approach, referring to the

EPIC model (Williams, 1995). The daily crop N demand is the difference between the crop N content and the ideal N content for that day, and estimated using the Eq. (B34). The optimal crop N concentration (C_{NB}) declines with increasing crop growth stage (Jones, 1983). It is calculated using Eq. (B35) in which bn_1, bn_2 and bn_3 are crop parameters calculated from crop-specific concentration of N in the plant at seedling, halfway through the season, and maturity, respectively.

$$UND_i = C_{NB,i} B_i - \sum_{k=1}^{i-1} UN_k \tag{B34}$$

$$C_{NB,i} = bn_1 + bn_2 \exp(-bn_3 HUI_i) \tag{B35}$$

where UND is the N demand rate of the crop (kg N ha^{-1} d^{-1}), UN is the actual N uptake rate (kg N ha^{-1} d^{-1}), and the subscript i refers to the day number.

N is taken up as NH_4^+ and NO_3^- by plants, considering both of the active process and passive process in the AHC. The amount of N that passively enters the plant (N_t^{Pass}) is determined by the plant transpiration rate and the concentration of N in the soil water that enters the plant. If passive N uptake is not enough to meet the plant demand, then active N uptake occurs. A rectangular hyperbola equation suggested by the RZWQM model (Ahuja et al., 2000) is used to estimate the rate of active N uptake (N_t^{Act}, kg N plant^{-1} d^{-1}):

$$N_t^{Act} = \mu_1 \frac{N_t^{Soil}}{\mu_2 + N_t^{Soil}} \tag{B36}$$

where N_t^{Soil} is the amount of N available in the soil layer (kg N ha^{-1}), μ_1 is the maximum proportion of N that can be removed from the soil (kg N plant^{-1} d^{-1}), and μ_2 the half maximum nitrogen-uptake amount for the species being simulated (kg N ha^{-1}). The total amount of additional nitrogen available to the plant through uptake is the sum of N_t^{Pass} and N_t^{Act}.

(7) *Solid adsorption*

The adsorption is assumed to be instantaneous (equilibrium approach) and can be described by a linear, Freundlich or Langmuir isotherm (Eq. B37). There is almost no adsorption for NO_3^-. Thus, the adsorption is only considered for NH_4^+ that tends to be absorbed on soil particle.

$$Q_k = \frac{k_{s,k} c_k^{\beta_k}}{1 + \eta_k c_k^{\beta_k}} \tag{B37}$$

where $k_{s,k}$ (cm^3 g^{-1}), β_k (-) and η_k (cm^3 g^{-1}) are empirical coefficients. When β_k=1, Eq. (B37) becomes the Langmuir equation, when η_k =0, it becomes the Freundlich equation, and when the η_k =0 and β_k=1, it represents the liner adsorption isotherm. There is no solid adsorption when $k_{s,k}$=0.

Annex C. Treatment for soil frost and thaw conditions

(1) ***Adjustment for soil hydraulic conductivity***

As soil water freezes below a soil temperature of 0°C, the soil hydraulic conductivity is further adjusted under frost conditions, as follows (Kroes and van Dam, 2003):

$$K^*(z) = f_{ST}(z)\left(K(z) - K_{\min}\right) + K_{\min} \qquad \text{(C1)}$$

$$f_{ST}(z) = \begin{cases} 1.0 & T \geq T_1 \\ \dfrac{T(z) - T_2}{T_1 - T_2} & T_2 < T(z) < T_1 \\ 0 & T < T_2 \end{cases} \qquad \text{(C2)}$$

where $K^*(z)$ is the adjusted hydraulic conductivity at depth z (cm d^{-1}), K_{min} is a very small hydraulic conductivity (cm d^{-1}) with a default value of 10^{-10} cm d^{-1}, $f_{ST}(z)$ is a correction factor for soil temperature at depth z, $T(z)$ is the soil temperature at depth z (°C), and T_1 and T_2 are the soil temperatures where reduction of hydraulic conductivity just begins and ends, respectively. The default values for T_1 and T_2 are taken as 0°C and -1°C.

(2) ***Soil thawing process: a simple approach***

In the AHC, a variable active-node method is proposed to describe the simulation zone (i.e. active zone) and simulating the fate of soil water and solute during the soil thawing period in a simple way (Xu et al., 2013). This is particularly designed for the initial season when upper soil layer fully thaws while underlying soil layer is in thawing processes (e.g., for spring wheat growth in Northwest China). The active zone corresponded to the upper fully thawed soil layer, which is bounded by the soil surface at the top and the upper boundary of frozen soil layer at the bottom. The rest nodes below are set as inactive nodes. The active zone depth (D_{act}, cm) is increased with soil thawing, estimated using Eq. (C3).

$$
\begin{aligned}
D_{act} &= a \cdot J^{b} + c \qquad && if\ D_{act} < D_{\max} \\
D_{act} &= D_{sp} \qquad && if\ D_{act} \geq D_{\max}
\end{aligned}
\tag{C3}
$$

where $D_{\max}$ is the maximum active zone depth (cm) and specified according to in-situ observation or experience, D_{sp} is the depth of whole simulation domain (cm), J is the day number after soil starts to thaw, c is the value of D_{act} in initial simulation, and a and b are empirical coefficients (-). Given that the thawing rate tended to increase with time, b should be larger than one. Meanwhile, a non-flux bottom boundary condition is defined for the active zone during thawing period, assuming that there is little water and solute exchange at the frozen interface. After the soil profile fully thaws, all nodes are activated and the bottom boundary condition is redefined as user-specified previously.

Annex D. EPIC crop growth module

The EPIC crop growth module (EPIC_CGM) considers leaf area development, light interception and conversion of intercepted light into biomass and yield, and the effects of temperature, water, and salt or nitrogen stress. The detailed calculation procedure is provided in the following parts.

Biomass: The solar radiation intercepted by crop leaf area is estimated with Beer's law (Monsi and Saeki, 1953):

$$PAR_{day} = 0.5 \cdot RA_{day} \cdot [1 - \exp(-k_l \cdot LAI)] \quad \text{(D1)}$$

where PAR_{day} is the intercepted photosynthetic active radiation on a given day (MJ m^{-2}), RA_{day} and $0.5 \cdot RA_{day}$ are respectively the total incident solar radiation (MJ m^{-2}) and incident photosynthetic active radiation, k_l is the light extinction coefficient, and LAI is leaf area index (-). The k_l varied with foliage characteristic, sun angle, row spacing and direction, and latitude. The default value of k_l used in the AHC (=0.65) is representative of crops with narrow row spacing, and a smaller value (0.4-0.6) might be suitable for wide row spacing and for tropical areas with higher sun angle (Williams et al., 1989).

The potential increase in biomass on a given day is estimated according to Monteith and Moss (1977), as follows:

$$\Delta B_a = RUE \cdot \Delta B_p = RUE \cdot PAR_{day} \cdot REG \quad \text{(D2)}$$

where ΔB_a and ΔB_p are the daily actual and potential increase in total biomass (kg ha^{-1}), respectively, RUE is the plant radiation-use efficiency ((kg ha^{-1})$\cdot$(MJ m^{-2})$^{-1}$), and REG is the crop growth regulating factor (the minimum stress factor) (-). The REG value is equal to the minimum stress factor of water-salt stress (α_{ws}) and temperature stress for salinity simulation, and that of water stress (α_w), nitrogen stress and temperature stress for nitrogen simulation. The calculation of α_w and α_{ws} can be found in Annex A. The stress factors of nitrogen (α_N) and temperature (α_T) are calculated using Eq. (D3) and Eqs. (D4-D5), respectively.

$$\alpha_T = \sin\left(\frac{\pi}{2}\left(\frac{T_{avg} - T_b}{T_{opt} - T_b}\right)\right) \tag{D3}$$

$$\alpha_N = \frac{N_{scale}}{N_{scale} + \exp\left(3.52 - 0.026 N_{scale}\right)} \tag{D4}$$

$$N_{scale} = 200\left[\frac{\sum_{k=1}^{i} UN_k}{(C_{NB})_i B_i} - 0.5\right] \tag{D5}$$

where *RUE* is sensitive to the atmospheric CO_2 level and affected by *VPD*. The equations of Stockle et al. (1992) are applied to adjust *RUE* for considering the effects of CO_2, as follows:

$$RUE^* = \frac{100CO_2}{CO_2 + \exp(bc_1 - bc_2(CO_2))} \tag{D6}$$

where bc_1 and bc_2 are crop shape factors. The *VPD* correction for adjusting *RUE* is accomplished in the equation:

$$\begin{aligned} RUE^{'} &= RUE^* - \Delta RUE_{slope}(VPD - VPD_{thr}) \quad &\text{if } VPD > VPD_{thr} \\ RUE^{'} &= RUE^* \quad &\text{if } VPD \le VPD_{thr} \end{aligned} \tag{D7}$$

where ΔRUE_{slope} is the rate of decline in *RUE* per unit increase in *VPD* ((kg ha^{-1})$\cdot$(MJ m^{-2})$^{-1}\cdot$ kPa^{-1}). Finally, the RUE' is substituted into Eq. (D2) to estimate the corrected biomass.

Leaf Area Index: The phonological development stage is controlled by heat unit accumulation. The heat unit index (*HUI*), representing the fraction of potential heat units accumulated in a given data, is calculated as follows:

$$HUI_i = \frac{\sum_{k=1}^{i} HU_k}{PHU} \tag{D8}$$

where HU is the heat units (ºC) on day i (equaling to average daily temperature minus base temperature), and PHU is the total potential heat units required for crop maturation (ºC). The value of HUI ranges from 0 at planting to 1 at physiological maturity.

LAI represents the level of canopy cover, and is estimated as a function of heat unit, crop stress and development stages using the equations:

$$\Delta LAI = (HUF_i - HUF_{i-1})LAI_{mx}(1-\exp(5(LAI_{i-1} - LAI_{mx})))\sqrt{REG_i} \tag{D9}$$

$$LAI_i = LAI_{i-1} + \Delta LAI \tag{D10}$$

where subscript i is the day number, Δ is the daily change, subscript mx refers to the maximum value possible for the crop, and HUF is the heat unit factor. The HUF is calculated as follows:

$$HUF_i = \frac{HUI_i}{HUI_i + \exp(ah_1 - ah_2 \cdot HUI_i)} \tag{D11}$$

where ah_1 and ah_2 are the shape coefficients for the corresponding crop. From the start of leaf decline till to the end of the growing season the LAI is estimated as follows:

$$LAI_i = LAI_c\left(\frac{1-HUI_i}{1-HUI_c}\right)^{\alpha} \tag{D12}$$

where α is a parameter governing the rate of decline in LAI, and the subscript c represents the day number of year when LAI starts declining.

Crop height: Crop height has a significant effect on the aerodynamic resistance in ET calculation. It can be directly specified as a function of the development stage, or estimated as follows:

$$H_{c,i} = H_{c,mx}\sqrt{HUF_i} \tag{D13}$$

where $H_{c,i}$ is the canopy height on day i (cm), and $H_{c,mx}$ is the maximum canopy height (cm).

Root system: The fraction of total biomass partitioned to the root system is 30-50% in seedlings and reduced to 5-20% in mature plants (Jones, 1985). This model decreases the fraction of total biomass in roots (fr_{root}) linearly from 0.4 at emergence to 0.2 at maturity, using the equation:

$$fr_{root} = 0.4 - 0.2HUI_i \tag{D14}$$

Root depth normally increases rapidly from the seeding depth to a specific maximum depth before maturity (Borg and Grimes, 1986). The daily increase in root depth is simulated as a function of heat unit index and potential root zone depth, as follows:

$$RD_i = 2.5(RD_{mx})(HUI_i) \quad \text{if } RD_i \le RD_{mx} \tag{D15}$$

where RD_i is the root depth on day i (cm) and RD_{mx} is the maximum root depth (cm). The vertical root distribution in soil profile is assumed to be a piecewise-linear function of root depth.

Crop yield: The actual crop yield is calculated using the harvest index concept:

$$Y_a = HI \cdot B_a \tag{D16}$$

where Y_a is the amount of the crop removed from the field (kg ha^{-1}), HI is the harvest index, and B_a is the actual aboveground biomass (kg ha^{-1}). For non-stressed conditions, the harvest index increases from 0 at planting to HI at maturity, and its value on each day of plant's growing season is simulated with the equations:

$$HIA_i = HI \cdot (\sum_{k=1}^{i} \Delta HUFH_k) \tag{D17}$$

$$HUFH_i = \frac{100HUI_i}{100HUI_i + \exp(11.1 - 10HUI_i)} \tag{D18}$$

where $HUFH$ is the heat unit factor affecting harvest index. Then, the HIA is corrected considering the effects of water, salinity and temperature, as follows:

$$HIA^* = \frac{HI}{1 + HI_{\min}(0.9 - WS) \cdot \max(0, \sin(\frac{\pi}{2}(\frac{HUI - 0.3}{0.3})))} \tag{D19}$$

where HI_{min} is the minimum harvest index allowed for plant under the water stress conditions. The WS is the water stress and equals to the ratio of actual crop transpiration to potential crop transpiration. Finally, HIA^* is substituted into Eq. (D16) to estimate the corrected crop yield.

Dormancy: The AHC assumes crops can go dormant in the winter season if the dormancy option is activated. During dormancy, transpiration is stopped and crops do not grow. The dates of beginning and end of dormancy are required to be specified by users. It is suggested that the dates should be determined based on the field observation or temperature. Such as in North China Plain, winter wheat will generally enter dormancy if the 5-day sliding average temperature drops below 0 ºC for the first time in winter season, and will come out of dormancy when that temperature above 0 ºC in the next spring (Ma et al., 2005).

Annex E. Treatment of bottom boundary conditions and lateral drainage

The treatment of the bottom conditions and lateral drainage in the AHC are kept same as that in the SWAP. Thus, only a brief introduction is provided here, and a more detailed description can be found in Kroes and van Dam (2003). The model provides eight options to prescribe the lower boundary conditions. The relevant description and equations are presented in Table E1. A simple, basic interaction between groundwater and a maximum of 5 surface water systems may be simulated. The drainage/infiltration (q_{drain}, cm d^{-1}) to/from each surface water system i is calculated as:

$$q_{drain,i} = \frac{\phi_{gwl} - \phi_{drain,i}}{\gamma_{drain,i}} \tag{E1}$$

where the drainage base $\phi_{drain,i}$ is equal to the surface water level of system i (cm below the soil surface), ϕ_{gwl} is the groundwater level (cm below the soil surface), $\gamma_{drain,i}$ is the drainage or infiltration resistance from system i (d). $\gamma_{drain,i}$ can be simply specified as a constant value, or estimated by using the drainage equations of Hooghoudt and Ernst. The latter one allows the more comprehensive evaluation of drainage design. The theory behind these equations is clearly described in Ritzema (1994). Five typical drainage situations are distinguished. For each of which the drainage resistance γ_{drain} can be calculated by equations given in Table E2.

Table E1. Eight options for the lower boundary condition

Code	Description	Type condition	Typical scale of application	Equation	Data input into model
1	Prescribe groundwater level (GWL)	Dirichlet	Field	$h_n = GWL - z_n - h_{resis}$	GWLs are given as function of time
2	Prescribe bottom flux (q_{bot})	Neumann	Region	$q_{bot} = q_{ng}$	q_{ng} is given as function of time
3	Calculate bottom flux from hydraulic head of deep aquifer	Cauchy	Region	$q_{bot} = (\phi_{aquif} - \phi_{avg})/c_{conf}$	ϕ_{aquif} and ϕ_{avg} is given as function of time; c_{conf} is required
4	Calculate bottom flux as function of groundwater level	Cauchy	Region	$q_{bot} = a_{qb} e^{b_{qb}\lvert\phi_{avg}\rvert}$	ϕ_{avg} is given as function of time
5	Prescribe soil water pressure head of bottom compartment (h_n)	Dirichlet	Field	$h_n = h_{ng}$	h_{ng} are given as function of time
6	Bottom flux equals zero	Neumann	Field	$q_{bot} = 0$	No data input required
7	Free drainage of soil profile	Neumann	Field	$\frac{\partial(h+z)}{\partial z} = 1$ thus: $q_{bot} = -K_n(h)$	No data input required
8	Free outflow at soil-air interface	Neumann	Field	when $h_n \le 0$, $q_{bot} = 0$; else when h_n increase to above zero, h_n is set to zero and drainage occurs	No data input required

Note: where h_{ng} (cm) and q_{ng} (cm d^{-1}) are the given pressure head and flux at the bottom of the soil profile, respectively. z_n is the position of bottom nodal point (negative, cm), and h_{resis} is the head difference between the groundwater level and hydraulic head of the bottom nodal point in the previous time step (cm). ϕ_{aquif} and ϕ_{avg} is the hydraulic head in the semi-confined aquifer (cm), ϕ_{avg} is the average groundwater level in the region (cm), and c_{conf} is the semi-confining layer resistance (d). h is the soil water pressure head (cm), z is the vertical coordinate (cm, positive upward), and $K_n(h)$ is the hydraulic conductivity of the bottom nodal point (cm d^{-1}).

Table E2. Drainage equations of Hooghoudt and Ernst

Code	Different conditions	Equation
1	Homogeneous profile, drain on top of impervious layer	$\gamma_{drain} = \dfrac{L^2_{drain}}{4K_{hprof}\left(\phi_{gwl} - \phi_{drain}\right)} + \gamma_{entr}$
2	Homogeneous profile, drain above impervious layer	$\gamma_{drain} = \dfrac{L^2_{drain}}{8K_{hprof}D_{eq} + 4K_{hprof}\left(\phi_{gwl} - \phi_{drain}\right)} + \gamma_{entr}$
3	Heterogeneous soil profile, drain at interface between both soil layers	$\gamma_{drain} = \dfrac{L^2_{drain}}{8K_{hbot}D_{eq} + 4K_{htop}\left(\phi_{gwl} - \phi_{drain}\right)} + \gamma_{entr}$
4	Heterogeneous soil profile, drain in bottom layer	$\gamma_{drain} = \left(\dfrac{\phi_{gwl} - \zeta_{\text{int}}}{K_{htop}} + \dfrac{\zeta_{\text{int}} - \phi_{drain}}{K_{vtop}}\right) + \dfrac{L^2_{drain}}{8K_{hbot}D_{eq}} + \dfrac{L_{drain}}{\pi\sqrt{K_{hbot}K_{vbot}}}\ln\left(\dfrac{D_{bot}}{u_{drain}}\right) + \gamma_{entr}$
5	Heterogeneous soil profile, drain in top layer	$\gamma_{drain} = \dfrac{\phi_{gwl} - \phi_{drain}}{K_{vtop}} + \dfrac{L^2_{drain}}{8K_{htop}D_{top} + 8K_{hbot}D_{bot}} + \dfrac{L_{drain}}{\pi\sqrt{K_{hbot}K_{vbot}}}\ln\left(\xi_{drain}\dfrac{\phi_{drain} - \zeta_{\text{int}}}{u_{drain}}\right) + \gamma_{entr}$

Note: L_{drain} the drain spacing (cm), K_{hprof} the horizontal saturated hydraulic conductivity above the drainage basis (cm d^{-1}), and γ_{entr} the entrance resistance into the drains and/or ditches (d).

D_{eq} is the equivalent depth (cm), K_{htop} and K_{hbot} the horizontal saturated hydraulic conductivity (cm d^{-1}) of upper and lower soil layer, respectively.

ζ_{int} the level of the transition (cm) between the upper and lower soil layer, K_{vtop} and K_{vbot} the vertical saturated hydraulic conductivity (cm d^{-1}) of the upper and lower soil layer, respectively, and D_{bot} is the contributing layer below the drain level (cm).

u_{drain} is the wet perimeter of the drain (cm), D_{top} equal to (ϕ_{drain} -ζ_{int}), and $\mathcal{E}_{\text{drain}}$ is the drain geometry factor (-).

Annex F. Supplementary material for the salinity and nitrogen cases

Table F1 Parameters and their ranges used in sensitivity analysis in the salinity case.

Parameter	Definition	Min	Max
θ_{r1}	Residual water content for material *i* (cm^3 cm^{-3})	0.02	0.08
θ_{s1}	Saturated water contents for material 1 (cm^3 cm^{-3})	0.38	0.48
θ_{si}	Saturated water contents for material *i* (cm^3 cm^{-3}) (*i*=2-4)	0.44	0.52
K_{si}	Saturated hydraulic conductivity for material *i* (cm d^{-1})	5	37
α_i	Empirical shape parameter in Eq. (2) for material *i* (-)	0.005	0.03
n_i	Empirical shape parameter in Eq. (2) for material *i* (-)	1.15	1.8
$L_{slt,i}$	Dispersion length for salt solute transport (cm)	6	22

Note: the subscript *i* is the number of soil material and equal to 1-4 in this case. Twenty-five parameters are selected for sensitive analysis.
The parameter range for calibration is kept same as that in sensitivity analysis.

Table F2 Parameters and their ranges used in sensitivity analysis in the nitrogen case.

Parameter	Definition	Min	Max
θ_{r1}	Residual water content for material *i* (cm^3 cm^{-3})	0.04	0.09
θ_{si}	Saturated water contents for material *i* (cm^3 cm^{-3})	0.38	0.52
K_{si}	Saturated hydraulic conductivity for material *i* (cm d^{-1})	5	37
α_i	Empirical shape parameter in Eq. (2) for material *i* (-)	0.005	0.03
n_i	Empirical shape parameter in Eq. (2) for material *i* (-)	1.15	1.8
$L_{\mathrm{amm},i}$	Dispersion length for NH_4^+ transport (cm)	6	22
$L_{\mathrm{nit},i}$	Dispersion length for NO_3^- transport (cm)	6	22

Note: the subscript *i* is the number of soil material and equal to 1-5 in this case. Thirty-five parameters are selected for sensitive analysis.
The parameter range for calibration is kept same as that in sensitivity analysis.

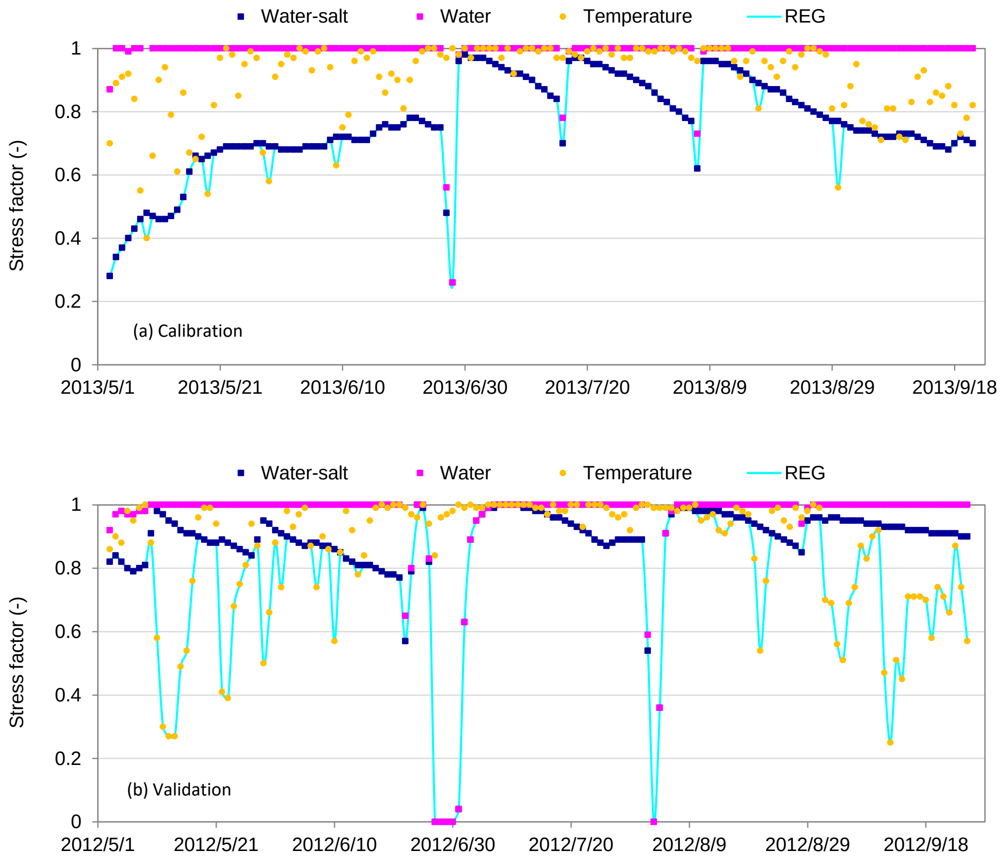

Figure. F1. Simulated stress factors of water-salt, water, temperature and the final regulating factor (REG) for maize growth during 2013 (a) and 2012 (b) in the salinity case

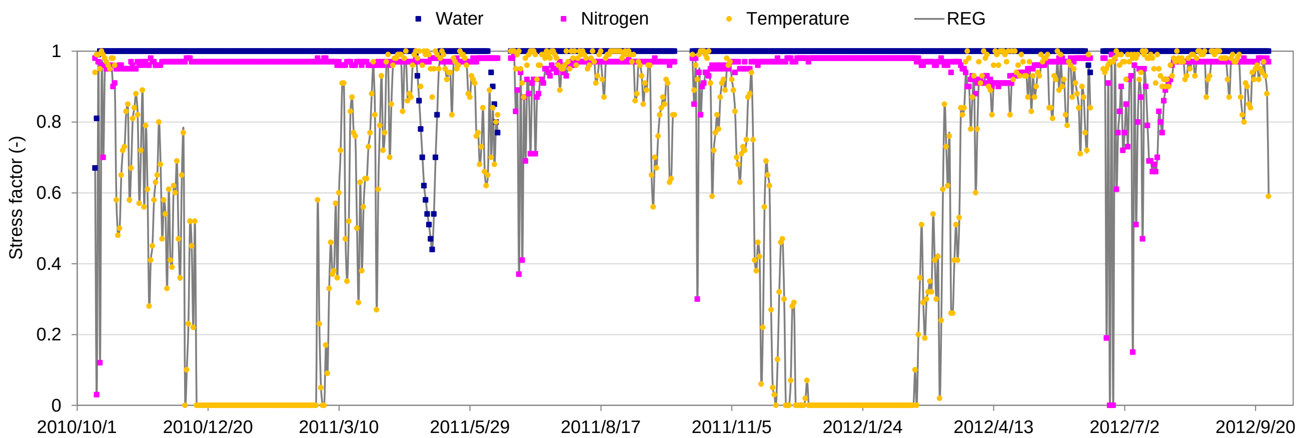

Figure. F2. Simulated stress factors of water, nitrogen, temperature and the final regulating factor (REG) for wheat-maize growth during 2010-2012 in the nitrogen case.

References

Ahuja, L.R., Rojas, K.W., Hanson, J.D., Shaffer, M.J. and Ma, L., 2000. The Root Zone Water Quality Model. Water Resources Publ., LLC, Highlands Ranch, CO, 372 pp.

Allen, R.G., Jensen, M.E., Wright, J.L. and Burman, R.D., 1989. Operational estimates of reference evapotranspiration. Agronomy Journal, 81(4): 650-662.

Allen, R.G., Pereira, L.S., Raes, D. and Smith, M., 1998. Crop evapotranspiration, Guidelines for computing crop water requirements. Irrigation and Drainage Paper 56, FAO, Rome, Italy.

Belmans, C., Wesseling, J.G. and Feddes, R.A., 1983. Simulation model of the water balance of a cropped soil: SWATRE. Journal of Hydrology, 63(3-4): 271-286.

Black, T.A., Gardner, W.R. and Thurtell, G.W., 1969. The prediction of evaporation, drainage, and soil water storage for a bare soil. Soil Science Society of America Journal, 33(5): 655-660.

Boesten, J. and Stroosnijder, L., 1986. Simple model for daily evaporation from fallow tilled soil under spring conditions in a temperate climate. Netherlands Journal of Agricultural Science, 34: 75-90.

Borg, H. and Grimes, D.W., 1986. Depth development of roots with time: an empirical description. Transactions of the ASAE, 29(1): 194-197.

Dirksen, C. and Augustijn, D.C., 1988. Root water uptake function for nonuniform pressure and osmotic potentials. Agronomy Abstract. ASA, Madison, WI: 185.

Feddes, R.A., Kowalik, P.J. and Zaradny, H., 1978. Simulation of field water use and crop yield, Simulation Monographs, Pudoc, Wageningen, The Netherlands, 189 pp.

Godwin, D.C., Jones, C.A., Ritchie, J.T., Vlek, P.L.G. and Youngdahl, L.G., 1984. The water and nitrogen components of the CERES models, Proceedings of the International Symposium on Minimum Data Set for Agrotechnology Transfer (ICRISAT (pp. 101-106).

Goodroad, L.L. and Keeney, D.R., 1984. Nitrous oxide production in aerobic soils under varying pH, temperature and water content. Soil Biology and Biochemistry, 16(1): 39-43.

Goudriaan, J., 1977. Crop micrometeorology: a simulation study. Pudoc.

Hansen, S., 2002. Daisy, a flexible soil-plant-atmosphere system model. Report. Dept. Agric.

Hansen, S., Jensen, H.E., Nielsen, N.E. and Svendsen, H., 1991. Simulation of nitrogen dynamics and biomass production in winter wheat using the Danish simulation model DAISY. Fertilizer research, 27(2-3): 245-259.

Homaee, M., Dirksen, C. and Feddes, R.A., 2002. Simulation of root water uptake: I. Non-uniform transient salinity using different macroscopic reduction functions. Agricultural Water Management, 57(2): 89-109.

Jarvis, N.J., 1989. A simple empirical model of root water uptake. Journal of Hydrology, 107(1-4): 57-72.

Jones, C.A., 1983. A survey of the variability in tissue nitrogen and phosphorus concentrations in maize and grain sorghum. Field Crops Research, 6: 133-147.

Jones, C.A., 1985. C4 Grasses and Cereals, 412 pp. John Wiley and Sons, Inc., New York.

Kroes, J.G. and van Dam, J.C., 2003. Reference Manual SWAP version 3.0.3, Alterra-report 773, Alterra, Green World Research, Wageningen.

Li, Y., White, R., Chen, D., Zhang, J., Li, B., Zhang, Y. et al., 2007. A spatially referenced water and nitrogen management model (WNMM) for (irrigated) intensive cropping systems in the North China Plain. Ecological Modelling, 203(3-4): 395-423.

Ma, Y.P., Wang, S.L. and Zhang, L., 2005. Study on improvement of WOFOST against overwinter of wheat in North China. Chinese Journal of Agrometeorology, 3: 145-149.

Maas, E.V. and Hoffman, G.J., 1977. Crop salt tolerance-current assessment. Journal of irrigation And Drainage Division, ASCE(103): 115-134.

McCown, R.L., Hammer, G.L., Hargreaves, J.N.G., Holzworth, D.P. and Freebairn, D.M., 1996. APSIM: a novel software system for model development, model testing and simulation in agricultural systems research. Agricultural Systems, 50(3): 255-271.

Monsi, M. and Saeki, T., 1953. Uber den Lictfaktor in den Pflanzengesellschaften und sein Bedeutung fur die Stoffproduktion. Japanese Journal of Botany, 14: 22-52.

Monteith, J.L., 1965. Evaporation and the environment. The State and Movement of Water in Living Organisims. Cambridge University Press: Swansea, pp. 205-234.

Monteith, J.L. and Moss, C.J., 1977. Climate and the Efficiency of Crop Production in Britain [and Discussion]. Philosophical Transactions of the Royal Society of London, Series B: Biological Sciences, 281(980): 277 -294.

Raes, D., Steduto, P., Hsiao, T.C. and Fereres, E., 2012. AquaCrop Version 4.0-Calculation procedures, FAO, Land and Water Division, Rome, Italy.

Reddy, K.R., Khaleel, R., Overcash, M.R. and Westerman, P.W., 1979. A nonpoint source model for land areas receiving animal wastes: II. Ammonia volatilization. Transactions of the ASAE, 22(6): 1398-1404.

Ritzema, H.P., 1994. Subsurface flow to drains. In 'Drainage principles and applications', H.P. Ritzema (Ed. in Chief), ILRI publication 16, second edition, Wageningen, p. 263-304.

Stockle, C.O., Williams, J.R., Rosenberg, N.J. and Jones, C.A., 1992. A method for estimating the direct and climatic effects of rising atmospheric carbon dioxide on growth and yield of crops: Part I—Modification of the EPIC model for climate change analysis. Agricultural Systems, 38(3): 225-238.

van Dam, J.C., Huygen, J., Wesseling, J.G., Feddes, R.A., Kabat, P., van Walsum, P.E.V. et al., 1997. Theory of SWAP Version 2.0. Simulation of Water Flow, Solute Transport and Plant Growth in the Soil-Water-Atmosphere-Plant Environment, Department of water resources, WAU, Report 71, technical Document 45, DLO Winand Staring Centre-DLO.

van Genuchten, M.T., 1987. A numerical model for water and solute movement in and below the root zone. United States Department of Agriculture Agricultural Research Service US Salinity Laboratory.

Williams, J.R., 1995. The EPIC model. In: V.P. Singh (Eds.), Computer Models of Watershed Hydrology. Water Resources Publications, Highlands Ranch, CO.

Williams, J.R., Jones, C.A., Kiniry, J.R. and Spanel, D.A., 1989. The EPIC crop growth model. Transactions of the ASAE, 32(2): 497-511.

Xu, C., Shaffer, M.J. and Al-kaisi, M., 1998. Simulating the impact of management practices on nitrous oxide emissions. Soil Science Society of America Journal, 62(3): 736-742.

Xu, X., Huang, G., Sun, C., Pereira, L.S., Ramos, T.B., Huang, Q. et al., 2013. Assessing the effects of water table depth on water use, soil salinity and wheat yield: Searching for a target depth for irrigated areas in the upper Yellow River basin. Agricultural Water Management, 125: 46-60.

Xu, X., Sun, C., Qu, Z., Huang, Q., Ramos, T.B., and Huang, G. et al., 2015. Groundwater recharge and capillary rise in irrigated areas of the upper Yellow River basin assessed by an agro-hydrological model. Irrigation and Drainage, doi: 10.1002/ird.1928.